RSC Advances

PAPER

View Article Online
View Journal | View Issue

Cite this: *RSC Adv.*, 2016, **6**, 110674

Synthesis, characterization and biological evaluation of cationic porphyrin–terpyridine derivatives†

Nuno M. M. Moura,*[abc] Catarina I. V. Ramos,[d] Inês Linhares,[e] Sérgio M. Santos,[f] M. Amparo F. Faustino,*[a] Adelaide Almeida,[e] José A. S. Cavaleiro,[a] Francisco M. L. Amado,[d] Carlos Lodeiro[bc] and M. Graça P. M. S. Neves*[a]

A simple access to a new series of cationic porphyrin–terpyridine derivatives is described. The key step to obtain the required neutral precursors as major products involved a Kröhnke type approach. The methodology allowed also the isolation of the respective benzoporphyrins and porphyrin–chalcone type derivatives, and in one case a new 2-(2,4-terpyridin-6-yl)-porphyrin. The quaternization of the pyridyl groups was performed in the presence of the adequate alkyl iodide affording the dicationic derivatives in excellent yields. All the new conjugates were fully characterised and it was found that the cationic isomers can be efficiently differentiated by ESI-MS, as their behaviour can be intensively studied by mass spectrometry. The new methylated cationic porphyrin–terpyridine derivatives demonstrate an ability to generate singlet oxygen and their efficacy to photoinactivate bioluminescent Gram-negative *E. coli* was evaluated. A reduction in the bioluminescence signal, up to 5.4 log, was obtained with the most efficient photosensitiser.

Received 17th October 2016
Accepted 7th November 2016

DOI: 10.1039/c6ra25373c

www.rsc.org/advances

Introduction

Porphyrins are receiving a lot of attention from the scientific community due to their high success in different fields like catalysis, development of advanced biomimetic models for photosynthesis, drugs, new electronic materials and sensors.[1] The richness of porphyrin applications is due to their synthetic versatility, thermal stability, large π-electron systems and photochemical and photophysical properties.[2,3] In particular, porphyrin-based macrocycles are being exploited with high success in medicine, namely as photosensitizers (PS) in photodynamic therapy of tumours (PDT)[4–7] or in photodynamic inactivation of microorganisms (PDI)[8–11] also known as antimicrobial photodynamic therapy (aPDT)[12,13] or antibacterial PDT.[14,15]

PDT and PDI are nowadays considered efficient alternatives to other techniques in the treatment of several diseases, such as tumours, age macular degeneration (AMD), skin disorders, and also in the inactivation of microorganisms, respectively.[4,16] The photodynamic process has as main advantages the fact that occur only in the illuminated region and the possibility to occur resistance is unlikely due to the non-specific killing mechanism.[5,17–19] Both therapies combine three key elements – light, oxygen and a photosensitiser (PS).[20] The combination of these non-toxic elements provide an efficient formation of high reactive oxygen species (ROS), such as the hydroxyl (˙OH) and superoxide ($O_2^{\bullet -}$) radicals and non-radical species, such as singlet oxygen ($^1O_2$) and hydrogen peroxide (H_2O_2).[21] These species are responsible for multi-targeted damage and destruction of living tissues. In porphyrin-mediated photodynamic inactivation (PDI), $^1O_2$ is in general considered the main damaging species.[22–24]

In last years, many studies proved the efficiency of cationic porphyrins as PS agents, in the microbial inactivation of viruses, fungi, protozoa, Gram-negative and Gram-positive bacteria.[25–30] The most promising studies are based on 5,10,15,20-tetrakis(1-alkylpyridinium-4-yl)porphyrin and its analogues where the charge is localized in the *meso*-substituents. Notwithstanding, there are few results in literature[31–34] of microorganism inactivation using cationic *meso*-tetraarylporphyrins bearing charges

[a]*Organic Chemistry Laboratory, QOPNA, Department of Chemistry, University of Aveiro, 3810-193 Aveiro, Portugal. E-mail: nmoura@ua.pt; gneves@ua.pt; faustino@ua.pt*

[b]*BIOSCOPE Research Team, UCIBIO, REQUIMTE, Departamento de Química, Faculdade de Ciências e Tecnologia, Universidade Nova de Lisboa, 2829-516 Caparica, Portugal*

[c]*ProteoMass Scientific Society, Madan Parque, Rua dos Inventores, 2825-182 Caparica, Portugal*

[d]*Mass Spectrometry Laboratory, QOPNA, Department of Chemistry, University of Aveiro, 3810-193 Aveiro, Portugal*

[e]*Department of Biology, CESAM, University of Aveiro, 3810-193 Aveiro, Portugal*

[f]*CICECO, Department of Chemistry, University of Aveiro, 3810-193 Aveiro, Portugal*

† Electronic supplementary information (ESI) available: Scheme S1: mechanistic pathway for the synthesis of compound **4**. Fig. S1–S66: NMR (1D and 2D) and HRMS spectra. Fig. S67: relationship between bioluminescence and viable counts of overnight cultures of recombinant *E. coli*. See DOI: 10.1039/c6ra25373c

in the beta-pyrrolic positions; the results already obtained show that this type of PSs is also very promising.

This fact, and our finding of an easy synthesis for porphyrin **1a** (see Fig. 1) bearing a terpyridine unit in the beta pyrrolic position,[35] prompted us to expand the studies to the syntheses of the analogues **1b** and **1c** in order to use them as templates for further cationization. So, herein, we report the synthesis and the characterization of a series of neutral and cationic porphyrins bearing terpyridine units in one of their beta-pyrrolic positions. In the course of the characterization of these compounds we found that isomer differentiation of the cationic compounds could be easily achieved by ESI-MS (electrospray mass spectrometry).

Additionally, their efficacy on the photoinactivation of bioluminescent *E. coli* was evaluated. The bioluminescent genetically transformed *E. coli* was selected as a model of Gram-negative bacteria to monitor in real-time photodynamic inactivation through bioluminescence measurement, thus avoiding the laborious and time-consuming conventional method of counting colony-forming units.

Results and discussion

Synthesis of neutral derivatives

The synthetic strategy to obtain the new β-pyrrolic cationic derivatives **6** and **7** (see Scheme 2) required the previous preparation of the corresponding neutral derivatives according with experimental work summarized in Scheme 1. The access to the new neutral porphyrins **1b** and **1c** bearing the terpyridine units in the β-pyrrolic positions involved the Kröhnke type approach described previously for the synthesis of porphyrin **1a**.[35] In this methodology the terpyridine moiety was built directly from the easy accessible 2-formyl-5,10,15,20-porphyrin (**TPP-CHO**)[36] by reaction with 2-acetylpyridine (5 equiv.) in the presence of ammonium acetate (8 equiv.) and $La(OTf)_3$ (20 mol%).[35] The procedure led to compound **1a** in good yield (45%) affording as minor compounds the benzoporphyrin **2a** (29%) and the porphyrin–chalcone **3a** (10%) (Table 1, entry 1).

Based on that synthetic strategy we envisaged, just by changing the 2-acetylpyridine by the adequate 3- and 4-acetylpyridine the syntheses of the new neutral terpyridine derivatives **1b** and **1c**.

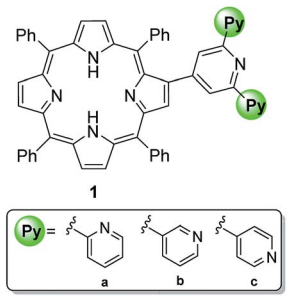

Fig. 1 Porphyrin–terpyridine derivatives **1a–c** used as template in this study.

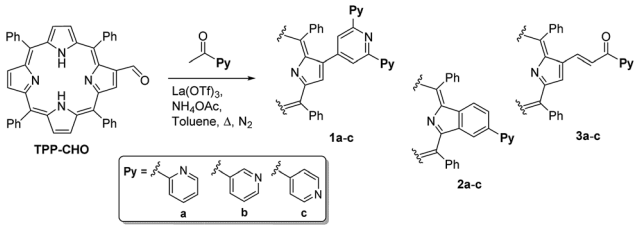

Scheme 1 Synthetic route to porphyrinic derivatives **1**, **2** and **3**.

Table 1 Products obtained from the reaction of 2-formyl-porphyrin (TPP-CHO) with acetylpyridines

Entry	Py	Time (h)	1 (%)	2 (%)	3 (%)	4 (%)	5 (%)
1[a]		3	45	29	10	—	—
2[a]		4	47	27	12	4	—
3[a]		6	16	7	33	—	7
4[b]		4	45	21	11	—	—
5[a]		6	18	8	36	—	2
6[b]		4	48	24	8	—	—

[a] Acetylpyridine (5 equiv.), NH_4OAc (8 equiv.), $La(OTf)_3$ (20 mol%), toluene, reflux. [b] Acetylpyridine (12 equiv.), NH_4OAc (14 equiv.), $La(OTf)_3$ (20 mol%), toluene, reflux.

In order to force the formation of the desired terpyridine **1a**, the reaction was repeated in the presence of 2-acetylpyridine during 4 h. The results summarized in Table 1 (entry 2) show that the expected derivatives **1a**, **2a** and **3a** were isolated in yields similar to our previously used conditions. However, a careful analysis of TLC data allowed us to detect a minor and more polar red product. After purification, the structure of this product, obtained in 4% yield, was established based on spectroscopic data (see infra and also ESI†) as the new 2-(2,4-diarylpyridin-6-yl)-5,10,15,20-tetraphenylporphyrin **4** (Fig. 2).

Attempts to improve compound **4** yield by increasing the reaction time were not successful. The formation of the new derivative **4** can be explained in a similar manner as the one proposed for derivative **1a**,[35] using as template the porphyrin–chalcone type derivative **3a** (see Scheme S1 of ESI†). However, instead of a Michael addition involving the 2-acetylpyridine that led to compound **1a**, an aldol condensation, followed by reaction with NH_3 occurs in the case of compound **4**.

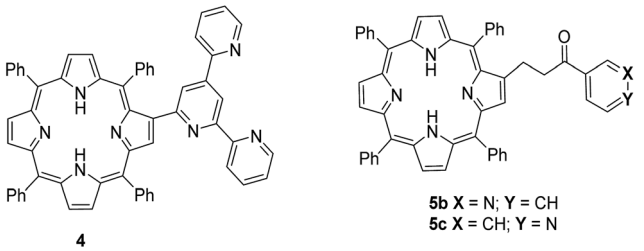

Fig. 2 Structures of compounds **4** and **5b**, **5c**.

Our first experiments with 3- and 4-acetylpyridine, were performed also in refluxing toluene, in the presence of 5 equiv. of these ketones, ammonium acetate and using $La(OTf)_3$ as catalyst as it was described for 2-acetylpyridine. However, under these conditions and even after 6 h of reaction, besides the large decomposition observed at the bottom of TLC, the main products isolated and structurally characterized (see below) after work up and chromatographic purification were the porphyrin–chalcone derivatives **3b** (33%) and **3c** (36%) instead of the desired 2-(terpyridin-4-yl)porphyrin derivatives **1b** (16%) and **1c** (18%), (Table 1, respectively entries 3 and 5). The low yields obtained for these porphyrin–terpyridines and also for the benzoporphyrins **2b** (7%) and **2c** (8%), also obtained from the same reactions, suggested that 3- and 4-acetylpyridines are less reactive than the 2-acetylpyridine.

For the reactions with 3- and 4-acetylpyridines, small amounts of new derivatives, identified as compounds **5b** (2%) and **5c** (7%) (Fig. 2), were also formed. The oxidative process involved in formation of terpyridine units is probably responsible by the appearance of these reduced porphyrin–chalcone derivatives.

In a further attempt to obtain the desired porphyrin derivatives **1b** and **1c** in higher yields, we decided to perform the reactions in the presence of a higher number of equivalents of the acetylpyridines (12 equiv.) and consequently of ammonium acetate and $La(OTf)_3$ (Table 1, entries 4 and 6). Under these conditions and after 4 h of reaction, we were able to isolate derivatives **1b** and **1c** as the main reactional products and in comfortable yields (45% and 48% respectively). Under these conditions the second most abundant products were the benzoporphyrin derivatives **2b**, **2c** (21 and 24%) followed by the porphyrin–chalcone type derivatives **3b**, **3c** (11 and 8%, respectively).

Structural characterization

The structural elucidation of all compounds involved the use 1D (^{1}H and ^{13}C spectra) and 2D [(^{1}H,^{1}H) COSY, NOESY, (^{1}H,^{13}C) HSQC and (^{1}H,^{13}C) HMBC] NMR techniques, high resolution mass spectrometry (HRMS-ESI) and UV-Vis spectroscopy.

In particular, the ^{1}H NMR of the new porphyrin–terpyridine derivatives **1b** and **1c** are consistent with β-substituted porphyrins showing the resonance of seven beta pyrrolic protons as multiplet at *ca.* δ 8.9 ppm. The resonances of the two protons from the central pyridyl show a characteristic singlet at *ca.* δ 7.8 ppm. The *meso*-phenyl protons appear as multiplets between *ca.* δ 7.1 and δ 8.3 ppm. The obtained ESI† mass spectra present a peak at *m*/*z* 846.3, corresponding to the molecular ion $[M + H]^+$, in agreement with the proposed structures for **1b** and **1c** (ESI, Fig. S1–S12†).

In the case of compounds **2a** and **2c** the ^{1}H NMR spectra show the resonances of only six β-pyrrolic protons, consistent with a benzoporphyrin derivative. The mass spectra obtained for both compounds show a peak at *m*/*z* 743.2 corresponding to the $[M + 2H]^{+\bullet}$ ion (see Fig. S13–S24 of ESI†).

Considering the ^{1}H NMR spectra of compounds **3b** and **3c** the most important features are the presence of a characteristic singlet at *ca.* δ 9.1 ppm corresponding to the resonance of the β-pyrrolic proton H-3 and an AB system at *ca.* δ 7.5 ppm due to the resonance of the two protons from the α,β-unsaturated ketone. The *trans* configuration of the chalcone moiety was clearly confirmed by the coupling constant ($J = 15.7$ Hz). The ^{13}C NMR spectra show a distinctive signal at *ca.* δ 191.0 ppm corresponding to the carbonyl carbon. Again, the mass spectra of compounds **3b** and **3c** present a peak, at *m*/*z* 746.3, that corresponds to the $[M + H]^+$ ion and confirms the proposed structures (Fig. S25–S36†).

The ^{1}H NMR patterns of the derivatives synthesized from 3- and 4-acetylpyridine are remarkably different. While the first ones show four signals in the range of approximately δ 9.0 ppm to δ 7.4 ppm, the derivatives from 4-acetylpyridine present two signals at *ca.* δ 8.7 and δ 7.7 (8.0 ppm for **1c**) ppm indicating highly symmetric structures. The 2D COSY experiments allowed the unequivocal attribution of the resonances of the protons from the pyridine moieties.

In all cases the presence of the two protons in the inner core of the porphyrinic macrocycle was confirmed by a singlet at *ca.* – δ 2.6 ppm.

The ^{1}H NMR of derivative **4** has a similar profile to the NMR obtained for its isomer **1a**, but it is indicative of a much less symmetric structure. This asymmetry is particularly noticeable in the signals generated by the resonances of the three pyridyl groups of the terpyridine moiety, namely in the central pyridyl where the resonances of the two protons generated two signals (δ 8.75 and δ 8.09 ppm) instead of only one singlet (*ca.* δ 7.5 ppm) as in the case of derivative **1a**. The mass spectrum of the compound **4** presents a peak at *m*/*z* 846.3 corresponding to the $[M + H]^+$ ion of the proposed structure (see ESI, Fig. S37–S42†).

The ^{1}H NMR of compounds **5** shows two multiplets at *ca.* δ 3.4 ppm and δ 3.3 ppm due to the resonance of the aliphatic protons from the reduced chain of the propanone moiety. The mass spectra of these compound are also in accordance with proposed structures, presenting a peak at *m*/*z* 748.3, corresponding to the $[M + H]^+$ ion (Fig. S43–S48 of ESI†).

Synthesis of cationic derivatives

The quaternisation of the pyridyl groups of the porphyrin–terpyridine derivatives **1** was performed in the presence of methyl iodide or ethyl iodide under conventional conditions as it is outlined in Scheme 2. A typical reaction was performed in *N*,*N*′-dimethylformamide (DMF) for 24 h at 40 °C in the presence of the respective 2-(2,6-diarylpyridin-4-yl)-porphyrin **1a–c** and using an excess of methyl or ethyl iodide. After that period, when methyl iodide was used, the reaction control by TLC confirmed the total conversion of all starting porphyrins **1** to more polar compounds that were identified as the corresponding dicationic products **6**. All the derivatives were obtained pure, in excellent yields (87–97%), directly from crystallization in CH_2Cl_2/hexane.

When ethyl iodide was used only the derivatives **7b** (96%) and **7c** (95%) were isolated, also in excellent yields and directly from crystallization in CH_2Cl_2/hexane. All attempts to ethylate the pyridine units of compound **1a** were not successful and only the starting porphyrin was recovered.

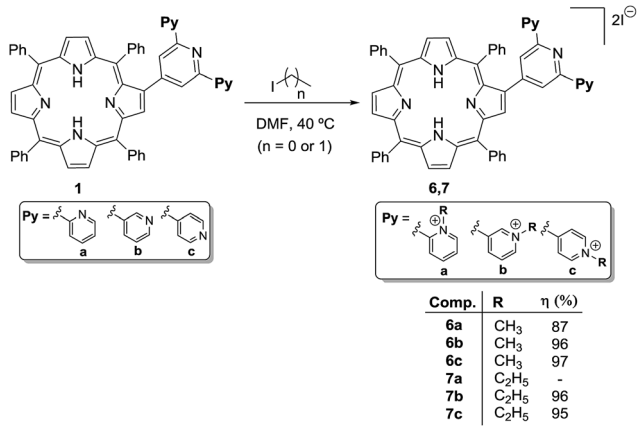

Comp.	R	η (%)
6a	CH_3	87
6b	CH_3	96
6c	CH_3	97
7a	C_2H_5	-
7b	C_2H_5	96
7c	C_2H_5	95

Scheme 2 Alkylation of porphyrin–terpyridine derivatives **1a–c**.

The proximity of the nitrogen atoms in this terpyridine moiety is probably compromising the nucleophilic attack on the more bulky ethyl iodide and it is why we were not able to isolate any *N*-alkylated derivative in this reaction.

It is worth to mention that all the attempts to alkylate the third pyridyl unit by increasing the reaction time or by using dimethyl sulphate as alkylating agent were not successful. This fact may be explained by the reduced basicity of the central pyridine unit after cationization of the other two pyridine units.

The structure of the alkylated derivatives **6a–c** and **7b**, **c** were confirmed by recording their ^{1}H-NMR, ^{13}C-NMR and mass spectra. In particular, the ^{1}H NMR spectra present a pronounced deviation for low fields of the signals in aromatic region, namely, the peaks generated by the resonances of the protons from the pyridine rings. The resonances of the protons from the methyl groups (**6a–c**) generated a distinctively singlet at *ca.* δ 4.5 ppm, while the resonances of protons from the ethyl chains (**7b**, **c**) generated two typically signals, a quartet at *ca.* δ 4.8 ppm and a triplet at *ca.* δ 1.7 ppm. The characteristic signal due to resonances of the inner N*H* protons appears, as expected, at high field at *ca.* δ −2.7 ppm (see ESI, Fig. S49–S66†).

Characterization of the cationic derivatives by electrospray mass spectrometry

In the course of the characterization of the obtained cationic compounds we found that we could easily differentiate these isomers by ESI-MS. These findings led us to investigate, in further detail, the gas-phase behavior of the neutral compounds **1** and of their corresponding methylated and ethylated counterparts, the cationic compounds **6** and **7**, respectively.

In the mass spectra of the neutral isomeric compounds **1**, the expected $[M + H]^+$ ions, *m*/*z* 846.4, were observed with high relative abundance. Higher abundant $[M + 2H]^{2+}$ ions, *m*/*z* 423.7, were also observed. Formation of $[M + 2H]^{2+}$ ions was already observed by us for neutral porphyrin–chalcone structures[37] and for neutral imidazole porphyrins and metalloporphyrins.[38] However, in the case of the imidazole-porphyrins and metalloporphyrins studied, the $[M + 2H]^{2+}$ ions showed lower abundance, when compared with the corresponding monoprotonated species.

For the methylated isomers, the compounds **6**, the expected doubly charged M^{2+} ions, *m*/*z* 437.8, were observed with high abundances. Triply charged species corresponding to $[M + H]^{3+}$ ions, *m*/*z* 292.2, were also identified in the case of compounds **6b** and **6c**, the abundance being higher for the former. As can be observed in Fig. 3 this species is absent in the mass spectra of isomer **6a** (*ortho*) allowing its differentiation from the other two isomers.

The absence of the triply charged species $[M + H]^{3+}$ for compound **6a** points to the occurrence of the protonation preferentially in the terpyridine moiety, since if it did occur in the core of the macrocycle, the formation of the $[M + H]^{3+}$ ions should also be observed for isomer **6a**. This behaviour was not unexpected because, as mentioned once, the sterical hindrance is higher in the case of the alkylated *ortho* isomers.

Monocharged ions, *m*/*z* 1002.3, corresponding to the formation of adducts with the iodide counter ion, $[M^{2+} + I^-]^+$, were observed for the *meta* isomer, compound **6b**. This characteristic feature allows the differentiation of this isomer and points to a preferential formation of its $[M + I^-]^+$ adduct. In order to understand this behavior, theoretical studies were performed for the terpyridine moieties. As it can be seen in Fig. 4 the stereochemistry of the *meta* isomer allows a closer approach of the iodide anion to the positive charges of the nitrogen atoms of the pyridinium cations, resulting in an increase of the coulombic attractive forces and consequently in a preferential formation of the $[M + I^-]^+$ adduct.

It is interesting to note that, besides the described species, a monocharged ion, at *m*/*z* 860.4, is also present for the *ortho* isomer. This ion is also diagnostic for the differentiation of this isomer and probably results from a reduction process involving the formation of the hypervalent radical ions $[M^{2+} + e^-]^+ = M^{+\bullet}$. Aromatic hypervalent pyridinium radicals, contrary to aliphatic ammonium hypervalent radicals, which are transient species,[39] are relatively stable due to charge delocalisation throughout the macrocycle. However, they fragment by loss of alkyl radicals forming neutral pyridyl functionalities, whenever this fragmentation is energetically favourable (Scheme 3). The formation and fragmentation of hypervalent ions by loss of alkyl

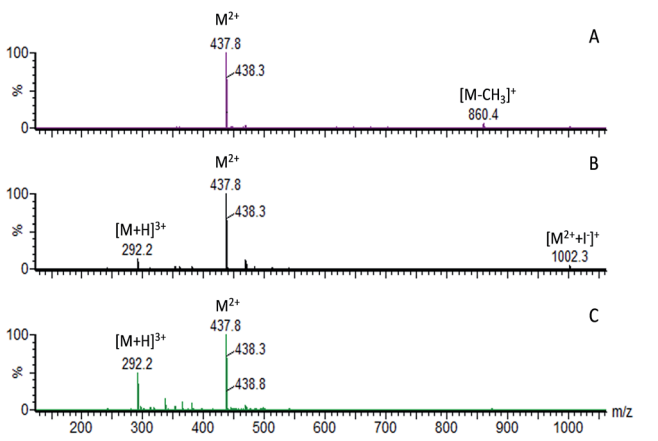

Fig. 3 Mass spectra of (A) compound **6a**; (B) compound **6b**; (C) compound **6c**.

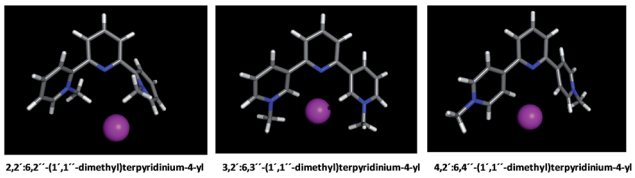

Fig. 4 Lowest energy conformations for the iodide adducts of terpyridine moieties of compounds **6a**, **6b** and **6c**; color code: blue – nitrogen; grey – carbon; white – hydrogen; purple – iodine.

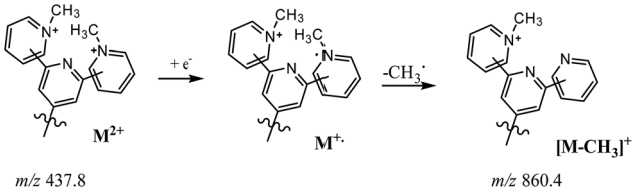

Scheme 3 Formation of the $[M - CH_3]^+$ ions from a methyl loss following a reduction process with formation of the hypervalent cation $M^{+\bullet}$.

radicals, in positive ion mode ESI-MS, was previously reported by us for other cationic porphyrins.[40,41]

The above mentioned processes leading to the formation of the $[M - CH_3]^+$ ion are favoured in the case of *ortho* isomer due to the higher sterical hindrance induced by the proximity of the methyl substituents.

In the case of the ethylated isomers 7, the *ortho* isomer could not be made probably due to the increased sterical hindrance caused by the longer alkyl chain. The gas phase behavior of the ethylated *meta* and *para* isomers is similar to the obtained for the corresponding methylated *meta* and *para* isomers, as it can be seen in Fig. 5.

ESI-MS proved to be a useful technique for the differentiation of the alkylated isomers through the formation of different diagnostic ions. The absence of the $[M + H]^{3+}$ ion and the formation of the monocharged $[M - CH_3]^+$ ion allowed the differentiation of the *ortho* isomer **6a** from the others two isomers. On the other hand, formation of the $[M + I^-]^+$ adducts is a feature that is specific of the *meta* alkylated isomers, **6b** and **7b**, enabling their differentiation from the *para* isomers, **6c** and **7c**.

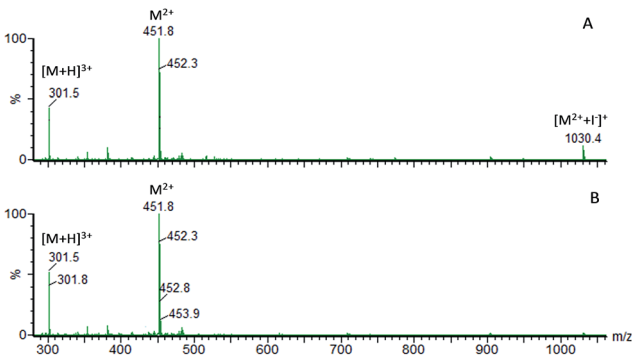

Fig. 5 Mass spectra of (A) compound **7b**; (B) compound **7c**.

Photophysical properties and biological evaluation

Singlet oxygen generation. In order to evaluate the potentiality of new materials for the photodynamic inactivation of bacteria, their ability to generate singlet oxygen should be previously estimated. In these studies, the ability to produce $^1O_2$ by the cationic porphyrins **6a–c** was qualitatively estimated using 1,3-diphenylisobenzofuran (DPiBF) as $^1O_2$ indicator.[42] The yellow DPiBF (with a maximum wavelength at 415 nm) reacts with $^1O_2$ generated by the combined action of light, PS and dissolved oxygen in a [4 + 2] cycloaddition affording a colourless *o*-dibenzoylbenzene. The decay of DPiBF absorption band at 415 nm allows to evaluate the ability of each porphyrin to generate $^1O_2$. As reference was used 5,10,15,20-tetrakis(1-methylpyridinium-4-yl)porphyrin (Tetra-Py$^+$-Me) that was proved to be an excellent singlet oxygen generator and efficient in the photodynamic inactivation of microorganisms.[43]

The results obtained with the cationic porphyrins (**6a–c**) are represented in Fig. 6 and confirm that all the studied porphyrins are able to cause a decay of DPiBF absorption within 10 min when irradiated with light at an irradiance of 4.0 mW cm^{-2}. Compounds **6a** and **6c** showed a distinctively aptitude to generate singlet oxygen when compared with **6b**; the efficiency of this derivative to generate $^1O_2$ generation is around 25% of the reference Tetra-Py$^+$-Me, while the others varied between ~70 and ~85%. These data demonstrate that the localisation of the positive charges could be a determinant factor for the $^1O_2$ generation. The results found allow to state that compounds **6** exhibit potentiality to be used as PS in the photodynamic inactivation of microorganisms.

Bioluminescence *versus* colony forming units of an overnight culture. The correlation between the colony-forming units (CFU) and the bioluminescence signal of *E. coli* was evaluated and a high correlation ($R = 0.9846$) between viable counts and the bioluminescence signal of overnight cultures was observed (Fig. S67, ESI†). Thus, the bioluminescence results reflect the viable bacterial abundance, allowing to obtain results in real time in a cost effective way. Consequently, the effect of bacterial photoinactivation by the porphyrin derivatives was assessed using the bioluminescent method.[44]

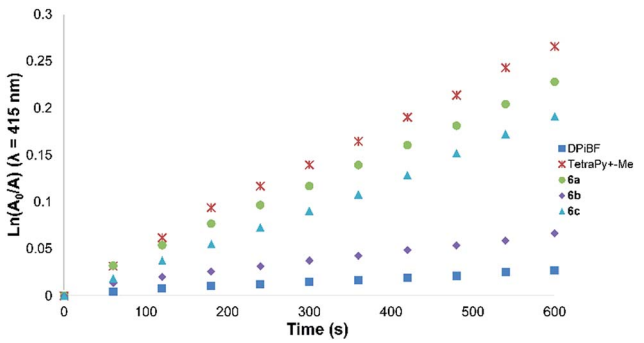

Fig. 6 Time dependent photodecomposition of DPiBF (50 μM) photosensitized by derivatives **6a–c** and Tetra-Py$^+$-Me in DMF/H_2O (9 : 1) upon irradiation with red light LEDs (654 nm ± 20 nm) with an irradiance of 4.0 mW cm^{-2} with and without porphyrin–terpyridine derivatives (0.5 μM).

Cationic β-functionalized *meso*-tetraarylporphyrins on the photoinactivation of bioluminescent *E. coli*. The results of the experiments carried out under PAR white light (380–700 nm) conditions (4.0 mW cm^{-2}) showed that the cationic porphyrins under study are able to cause a decrease in the bioluminescent signal emitted by *E. coli*. In the three independent experiments (Fig. 7) the compound **6a** was the most effective derivative causing a reduction of *ca.* 2.4 log on bioluminescence signal after 270 min of irradiation. At same light conditions, compounds **6b** and **6c** were less effective causing a reduction of *ca.* 1.4 log and *ca.* 2.0 log on bacterial bioluminescence, respectively (Fig. 7). The inactivation profile was similar in the three independent assays, even with different bacteria densities (Fig. 7).

The better efficiency of **6a** and **6c** when compared with **6b** is probably associated with their much higher ability to produce $^1O_2$. However, the production of $^1O_2$ even for **6b** compound is considered to be enough to inactivate the bacteria when compared with other PS from previous studies.[45] So other factors are also contributing for this inactivation profile such as structural features which can affect the adequate conformation to interact with the bacterial targets. In fact, the terpyridine units in the β-pyrrolic position differ in the position of the nitrogen linked to central pyridyl. Probably the charge distribution in **6a** and **6c** turn these molecules more accessible to interact with the external structure of the bacteria when compared with the derivative **6b**. A possible explanation can be due to the closer approach of the iodide anion to the positive charges of the nitrogen atoms of the pyridinium cations in derivative **6b** as it was verified by mass spectrometry studies.

The results of control samples show that the viability of the recombinant bioluminescent *E. coli* was not affected either by irradiation (light control) or by any of the compounds tested (dark control). The reduction of cell viability observed after irradiation of the treated samples is clearly due to the photosensitisation effect of the cationic porphyrins as it was demonstrated by the three independent experiments of photoinactivation performed (Fig. 7).

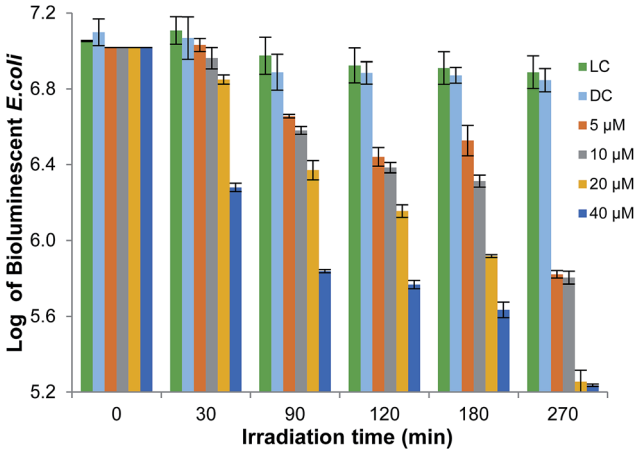

Fig. 8 Bioluminescence monitoring of *E. coli* treated with **6a** at 5, 10, 20 and 40 μM after 30, 90, 120, 180 and 270 min of irradiation with white light at an irradiance of 4.0 mW cm^{-2}. The values are expressed as the means of three independent experiments; error bars indicate the standard deviation; DC dark control; LC light control.

In order to evaluate the effect of PS concentration on the *E. coli* photoinactivation efficiency, the most effective cationic porphyrin **6a** was irradiated using the same light conditions (4.0 mW cm^{-2}) at different final concentrations of 5, 10, 20 and 40 μM (Fig. 8). The photoinactivation efficiency of compound **6a** increases with the PS concentration but it seems to reach a plateau after 270 min of irradiation.

Knowing that the efficiency of the photoinactivation process can be significantly affected by the light irradiance[44,46] we decided to evaluate the efficacy of compound **6a** at 20 μM but at a higher light irradiance (150 mW cm^{-2}). The results depicted in Fig. 9 show that the increase of light irradiance from 4.0 to

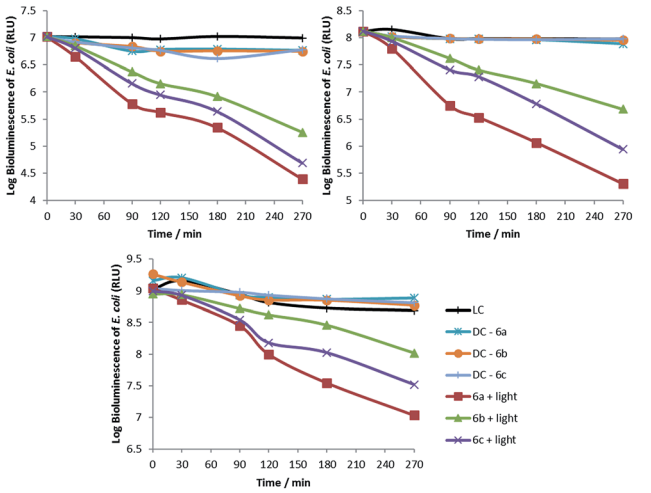

Fig. 7 Bioluminescence monitoring of *E. coli* treated with derivatives **6a–c** at 20 μM after 30, 90, 120, 180 and 270 min of irradiation with PAR white light at an irradiance of 4.0 mW cm^{-2} in three independent experiments with different bacteria density; DC dark control; LC light control.

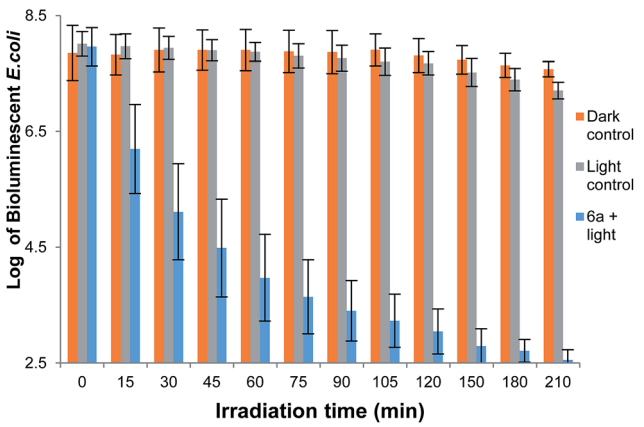

Fig. 9 Percentual of bioluminescence monitoring of *E. coli* treated with **6a** at 20 μM during 120 min of irradiation with white light at an irradiance of 150 mW cm^{-2}. The values are expressed as the means of three independent experiments; error bars indicate the standard deviation.

150 mW cm^{-2} caused a significant effect on the efficiency of **6a** to photoinactivate *E. coli*.

At this irradiance of 150 mW cm^{-2} and just after 30 min (270 J cm^{-2}), it was observed a reduction on the bioluminescence signal of 2.9 log, a value higher than the 2.4 log reduction obtained for the same compound when exposed to white light (PAR white light) at an irradiance of 4.0 mW cm^{-2} during 270 min (64.8 J cm^{-2}). The porphyrin **6a** reached reductions of the bioluminescence signal of 4.0 log after 60 min of irradiation and of 5.4 log after 210 min. According to the American Society for Microbiology, any new approach must achieve a reduction of at least 3 $\log_{10}$ CFU (killing efficiency of 99.9% or more) to be termed antimicrobial or antibacterial, which indicate that **6a** compound is an effective PS.[47,48] Control samples did not show significant variation in the emission of bioluminescence, indicating that light alone (light control) or **6a** at the studied concentration of 20 μM in the dark (dark control) do not affect bioluminescent *E. coli* viability.

Conclusions

New neutral porphyrin–terpyridine derivatives were efficiently prepared by reaction of 2-formyl-5,10,15,20-porphyrin with the appropriate acetylpyridine in the presence of ammonium acetate catalysed by $La(OTf)_3$. Secondary compounds were also isolated, the respective benzoporphyrins and porphyrin chalcones type derivatives. The studied conditions allowed also to isolate for the first time a 2-(2,4-terpyridin-6-yl)-porphyrin derivative. Two of the pyridine moieties in the terpyridine derivatives **1** were efficiently quaternised with methyl or ethyl iodide leading, in general, to the formation of the respective dicationic derivatives.

A detailed characterization on gas phase of the neutral and cationic porphyrin–terpyridine derivatives using electrospray mass spectrometry demonstrated that ESI-MS is a useful and efficient technique to differentiate the alkylated isomers due to the formation of different diagnostic ions.

The ability of the methylated terpyridine derivatives **6** to generate singlet oxygen was evaluated and confirmed their potential to be used as PSs. The photoinactivation of bioluminescent *E. coli* in the presence of these photosensitisers showed that the PS concentration, oxygen singlet efficiency, the distribution of the charge in the porphyrin core, light irradiance are important parameters to be taken into consideration.

Experimental section

General remarks

^1H and ^{13}C solution NMR spectra were recorded on Bruker Avance 300 (300.13 and 75.47 MHz, respectively), 500 (500.13 and 125.76 MHz, respectively) and 700 (700.13 MHz) spectrometers. $CDCl_3$, CD_3OD and DMSO-d_6 were used as solvent and tetramethylsilane (TMS) as internal reference; the chemical shifts are expressed in δ (ppm) and the coupling constants (J) in Hertz (Hz).

Unequivocal ^1H assignments were made using 2D COSY ($^1H/^1H$), while ^{13}C assignments were made on the basis of 2D HSQC ($^1H/^{13}C$) and HMBC (delay for long-range J C/H couplings were optimized for 7 Hz) experiments. Mass spectra were recorded using MALDI TOF/TOF 4800 Analyzer, Applied Biosystems MDS Sciex, with $CHCl_3$ as solvent and without matrix. Mass spectra HRMS were recorded on a LTQ Orbitrap XL mass spectrometer (Thermo Fischer Scientific, Bremen, Germany) using $CHCl_3$ as solvent. The UV-Vis spectra were recorded on an UV-2501PC Shimadzu spectrophotometer using DMF as solvent. Preparative thin-layer chromatography was carried out on 20 × 20 cm glass plates coated with silica gel (0.5 mm thick). Column chromatography was carried out using silica gel (Merck, 35–70 mesh). Analytical TLC was carried out on precoated sheets with silica gel (Merck 60, 0.2 mm thick).

All the chemicals were used as supplied. Solvents were purified or dried according to the literature procedures.[49]

Synthesis

Synthesis of the porphyrin precursor TPP-CHO. The 2-formyl-5,10,15,20-tetraphenylporphyrin **TPP-CHO** was prepared from 5,10,15,20-tetraphenylporphyrinatocopper(II), *N*,*N*′-dimethylformamide (DMF) and phosphorus oxychloride ($POCl_3$), according to literature procedure.[36]

Synthesis of the beta functionalized *meso*-tetraarylporphyrins 1–5: general procedure. To a solution of the appropriate acetylpyridine (5.0 or 12.0 equiv.) in dry toluene (1 mL) was added ammonium acetate (8.0 or 14 equiv.) and the mixture was stirred for 30 min at room temperature. After this time, 2-formyl-5,10,15,20-tetraphenylporphyrin **1** and $La(OTf)_3$ (20 mol%) were added to the mixture and it was heated at reflux in the range of 3–6 h. After cooling, the reaction mixture was washed with water and extracted with dichloromethane. The organic phase was dried (Na_2SO_4) and the solvent was evaporated under reduced pressure. The crude mixture was submitted to column chromatography (silica gel) using CH_2Cl_2 as eluent. The fractions obtained were full characterized by NMR, mass and UV-Vis techniques. The reactional conditions and yields are summarized in Table 1.

The characterization of compounds **1a**, **2a** and **3a** were performed by UV-vis, ^1H NMR and mass spectrometry and all the experimental data are in agreement with the described literature data.[35]

2-[3,2′:6,3″-Terpyridin-4-yl]-5,10,15,20-tetraphenylporphyrin, ***1b.*** ^1H NMR (500 MHz, $CDCl_3$): δ 9.31 (2H, d, $J = 1.7$ Hz, H-2″), 8.91 and 8.89 (2H, AB, $J = 4.8$ Hz, H-β), 8.85–8.83 (4H, m, H-β), 8.80 (1H, d, $J = 4.7$ Hz, H-β), 8.71 (2H, dd, $J = 1.7$ and 4.8 Hz, H-6″), 8.45 (2H, dt, $J = 1.7$ and 8.1 Hz, H-4″), 8.28–8.23 (6H, m, H-*o*-Ph), 8.02–8.01 (2H, m, H-*o*-Ph), 7.81–7.75 (9H, m, H-*m*,*p*-Ph), 7.73 (2H, s, H-3′ and H-5′), 7.47 (2H, ddd, $J = 0.6$, 4.8 and 8.1 Hz, H-5″), 7.17–7.14 (3H, m, H-*m*,*p*-Ph), −2.61 (2H, s, N*H*) ppm. ^{13}C NMR (125 MHz, $CDCl_3$): δ 153.4 (C-3″), 149.9 (C-6″), 149.5, 148.4 (C-2″), 142.2, 142.0, 141.7, 140.6, 138.9, 135.7, 134.7, 134.6 (C-4″), 134.5, 132.9–130.0 (C-β), 128.1, 128.0, 127.9, 126.9, 126.8, 126.2, 123.6 (C-5″), 121.26 (C-3′ and C-5′), 120.70, 120.66, 120.4, 120.3 ppm. UV-Vis (DMF): λ_{max} (log ε) 420 (5.43), 516 (4.21), 552 (3.80), 595 (3.63), 648 (3.55) nm. HRMS-ESI(+): *m*/*z* calcd for $C_{59}H_{40}N_7$ 846.33397 $[M + H]^+$; 846.33460 found.

2-[4,2′:6,4″-Terpyridin-4-yl]-5,10,15,20-tetraphenylporphyrin, ***1c***. ^{1}H NMR (500 MHz, $CDCl_3$): δ 8.92 and 8.89 (2H, AB system, J = 4.8 Hz, H-β), 8.85–8.83 (4H, m, H-β), 8.80–8.78 (5H, m, H-β, H-2″ and H-6″), 8.27–8.22 (6H, m, H-*o*-Ph), 8.02 (4H, dd, J = 1.6 and 4.6, H-3″ and H-5″), 8.00–7.97 (2H, m, H-*o*-Ph), 7.81 (2H, s, H-3′ and H-5′), 7.80–7.74 (9H, m, H-*m*,*p*-Ph), 7.11–7.10 (3H, m, H-*m*,*p*-Ph), −2.63 (2H, s, N*H*) ppm. ^{13}C NMR (125 MHz, $CDCl_3$): δ 153.3 (C-2′), 150.7, 150.5 (C-2″ and C-6″), 149.8, 146.2 (C-4″), 142.1, 142.0, 141.7, 140.5, 135.7 (C-3″ and C-5″), 134.6, 134.5, 133.1–130.0 (C-β), 128.1, 128.0, 127.9, 126.9, 126.8, 126.2, 122.4, 121.2 (C-3′ and C-5′), 120.8, 120.6, 120.5, 120.4 ppm. UV-Vis (DMF): λ_{max} (log ε) 421 (5.38), 516 (4.18), 552 (3.69), 592 (3.46), 651 (3.37) nm. HRMS-ESI(+): m/z calcd for $C_{59}H_{40}N_7$ 846.33397 $[M + H]^+$; 846.33450 found.

2^2-(Pyridin-3-yl)-5,10,15,20-tetraphenylbenzo[b]porphyrin, ***2b***. ^{1}H NMR (700 MHz, $CDCl_3$): δ 9.04 (1H, d, J = 1.4 Hz, H-2″), 8.93 (1H, d, J = 4.9 Hz, H-β), 8.91 (1H, d, J = 4.9 Hz, H-β), 8.85 (1H, d, J = 4.9, H-β), 8.84 (1H, d, J = 4.9 Hz, H-β), 8.74 (2H, AB system, J = 4.9 Hz, H-β), 8.64 (1H, dd, J = 1.4 and 4.6 Hz, H-6″), 8.24–8.21 (8H, m, H-*o*-Ph), 8.03 (1H, dt, J = 1.4 and 7.9 Hz, H-4″), 7.95–7.92 (2H, m, H-*m*,*p*-Ph), 7.86–7.75 (12H, m, H-*m*,*p*-Ph, H-1′ and H-3′), 7.35 (1H, ddd, J = 0.6, 4.6 and 7.9 Hz, H-5″), 7.29 (1H, d, J = 8.1 Hz, H-4′), −2.65 (2H, s, N*H*) ppm. ^{13}C NMR (125 MHz, $CDCl_3$): δ 160.1 (C-3″), 154.8, 151.7 (C-2″), 149.7, 148.6, 147.9, 147.0, 143.1, 142.2, 142.0, 141.9, 140.2, 138.9, 138.0, 135.0, 134.8, 134.5, 134.1, 134.0, 133.9, 133.6, 132.6, 128.7, 128.3, 128.0, 127.9, 127.8, 127.7, 127.3, 127.0, 126.8, 126.8, 123.3, 121.3, 121.2, 117.8, 117.7, 116.7 ppm. UV-Vis (DMF): λ_{max} (log ε) 425 (5.46), 517 (4.27), 593 (3.75) nm. HRMS-ESI(+): m/z calcd for $C_{53}H_{37}N_5$ 743.30490 $[M + 2H]^{+\bullet}$; 743.29159 found.

2^2-(Pyridin-4-yl)-5,10,15,20-tetraphenylbenzo[b]porphyrin, ***2c***. ^{1}H NMR (700 MHz, $CDCl_3$): δ 8.94 (1H, d, J = 4.9 Hz, H-β), 8.92 (1H, d, J = 4.9 Hz, H-β), 8.86 (1H, d, J = 4.9 Hz, H-β), 8.84 (1H, d, J = 4.9 Hz, H-β), 8.74 (2H, AB system, J = 4.9 Hz, H-β), 8.67–8.66 (2H, m, H-2″ and H-6″), 8.25–8.21 (8H, m, H-*o*-Ph), 7.95–7.90 (2H, m, H-*m*,*p*-Ph), 7.86–7.53 (12H, m, H-*m*,*p*-Ph, H-1′ and H-3′), 7.68–7.66 (2H, m, H-3″ and H-5″), 7.31 (1H, d, J = 8.2 Hz, H-4′), −2.67 (2H, s, N*H*) ppm. ^{13}C NMR (125 MHz, $CDCl_3$): δ 160.0, 154.9, 151.4, 150.1, 146.4, 143.1, 142.2, 141.9, 141.8, 138.9, 138.1, 134.5, 134.1, 133.6, 132.6, 128.7, 128.4, 128.1, 127.9, 127.8, 127.3, 127.1, 126.84, 126.80, 121.4, 121.3, 117.9, 117.8, 117.1 ppm. UV-Vis (DMF): λ_{max} (log ε) 426 (4.84), 517 (4.22), 592 (3.66) nm. HRMS-ESI(+): m/z calcd for $C_{53}H_{37}N_5$ 743.30490 $[M + 2H]^{+\bullet}$; 743.29054 found.

2-[3-Oxo-3-(pyridin-3-yl)prop-1-en-1-yl]-5,10,15,20-tetraphenylporphyrin, ***3b***. ^{1}H NMR (300 MHz, $CDCl_3$): δ 9.09–9.07 (2H, m, H-3 and H-2″), 8.85–8.75 (7H, m, H-β and H-6″), 8.26–8.24 (2H, m, H-*o*-Ph), 8.21–8.19 (4H, m, H-*o*-Ph), 8.14 (1H, dt, J = 1.9 and 7.9 Hz, H-4″), 8.08–8.05 (2H, m, H-*o*-Ph), 7.84–7.72 (9H, m, H-*m*,*p*-Ph), 7.59–7.57 (3H, m, H-*m*,*p*-Ph), 7.49–7.44 (3H, m, H-5″, H-1′ and H-2′), −2.56 (2H, s, N*H*) ppm. ^{13}C NMR (125 MHz, $CDCl_3$): δ 190.8 (C═O), 152.6, 149.8, 142.6, 142.1, 141.9, 141.7, 141.5, 136.1, 134.6, 134.55, 134.1, 133.9, 132.5–130.2 (C-β), 128.5, 128.1, 127.9, 127.1, 126.9, 129.8, 124.4, 123.5, 120.8, 120.5, 120.4, 120.3 ppm. UV-Vis (DMF): λ_{max} (log ε) 437 (4.71), 526 (4.24), 566 (3.97), 605 (3.86), 666 (2.86) nm. HRMS-ESI(+): m/z calcd for $C_{52}H_{36}N_5O$ $[M + H]^+$ 746.29144; 746.29051 found.

2-[3-Oxo-3-(pyridin-4-yl)prop-1-en-1-yl]-5,10,15,20-tetraphenylporphyrin, ***3c***. ^{1}H NMR (300 MHz, $CDCl_3$): δ 9.10 (1H, s, H-3), 8.86–8.77 (7H, m, H-β, H-2″ and H-6″), 8.73 (1H, d, J = 4.9 Hz, H-β), 8.25–8.17 (6H, m, H-*o*-Ph), 8.06–8.03 (2H, m, H-*o*-Ph), 7.84–7.72 (9H, m, H-*m*,*p*-Ph), 7.61–7.59 (2H, m, H-3″ and H-5″), 7.55–7.53 (3H, m, H-*m*,*p*-Ph), 7.42 and 7.37 (2H, AB system, J = 15.7 Hz, H-1′ and H-2′), −2.56 (2H, s, N*H*) ppm. ^{13}C NMR (125 MHz, $CDCl_3$): δ 192.0 (C═O), 151.0, 150.6, 147.8, 147.2, 146.8, 146.5, 145.8, 144.9, 143.6, 142.1, 141.9, 141.6, 141.4, 139.2, 138.9, 134.6, 134.1, 132.7–130.1 (C-β), 129.0, 128.9, 128.8, 128.64, 128.57, 128.4, 128.1, 127.9, 127.1, 126.9, 126.8, 124.4, 122.1, 121.7, 1212, 120.9, 120.5, 120.4, 120.2 ppm. UV-Vis (DMF): $\lambda_{máx}$ (log ε) 434 (4.89), 526 (3.97), 570 (3.62), 604 (3.52), 665 (1.95) nm. HRMS-ESI(+): m/z calcd for $C_{52}H_{36}N_5O$ $[M + H]^+$ 746.29144; 746.29031 found.

2-[2,2′:4,2″-Terpyridin-6-yl]-5,10,15,20-tetraphenylporphyrin, ***4***. ^{1}H NMR (700 MHz, $CDCl_3$): δ 9.05 (1H, s, H-3), 8.87–8.82 (5H, m, H-β), 8.76–8.73 (4H, m, H-β, H-6″, H-6‴ and H-3′), 8.37 (1H, d, J = 8.1 Hz, H-3‴), 8.26 (2H, dd, J = 1.6 and 7.6 Hz, H-*o*-Ph), 8.24–8.20 (4H, m, H-*o*-Ph), 8.09 (1H, d, J = 1.5 Hz, H-5′), 7.98 (2H, d, J = 6.0 Hz, H-*o*-Ph), 7.95 (1H, dt, J = 1.0 and 7.7 Hz, H-3″), 8.40 (1H, dt, J = 1.8 and 7.8 Hz, H-4″), 7.78–7.70 (10H, m, H-*m*,*p*-Ph and H-4‴), 7.34 (1H, ddd, J = 1.1, 4.7 and 7.5 Hz, H-5‴), 7.31 (1H, ddd, J = 1.0, 4.9 and 7.7 Hz, H-5″), 7.04–7.02 (1H, m, H-*m*-Ph), 6.97 (2H, t, J = 7.8 Hz, H-*m*-Ph), −2.58 (2H, s, N*H*) ppm. ^{13}C NMR (75 MHz, $CDCl_3$): δ 157.9, 156.1, 155.7, 155.0, 149.9, 149.0 (C-6″ and C-6‴), 146.4, 142.34, 142.26, 141.9, 140.7, 136.8 (C-4″), 136.6 (C-4″), 135.7, 134.6 (C-3), 132.2–130.1 (C-β), 127.7, 127.2, 126.8, 126.64, 126.61, 125.8 (C-β), 123.5 (C-5′), 121.8 (C-3‴), 121.3, 121.2 (C-3″), 120.4, 120.2, 120.0, 115.6 (C-3′) ppm. UV-Vis (DMF): λ_{max} (log ε) 420 (5.46), 517 (4.18), 552 (3.72), 595 (3.62), 650 (3.52) nm. HRMS-ESI(+): m/z calcd for $C_{59}H_{40}N_7$ 846.33397 $[M + H]^+$; 846.33411 found.

2-[3-Oxo-3-(pyridin-3-yl)propan-1-yl]-5,10,15,20-tetraphenylporphyrin, ***5b***. ^{1}H NMR (300 MHz, $CDCl_3$): δ 9.01 (1H, d, J = 1.6 Hz, H-2″), 8.78 (2H, AB system, J = 4.9 Hz, H-β), 8.74 (1H, d, J = 4.9 Hz, H-β), 8.69–8.67 (3H, m, H-β), 8.56–8.53 (2H, m, H-β and H-3), 8.14–8.04 (9H, m, H-*o*-Ph and H-4″), 7.69–7.56 (m, 12H, H-*m*,*p*-Ph), 7.30 (1H, dd, J = 4.8 and 8.0, Hz, H-5″), 3.42–3.36 (2H, m, H-2′), 3.31–3.26 (2H, m, H-1′), −2.84 (2H, s, N*H*) ppm. ^{13}C NMR (125 MHz, $CDCl_3$): δ 197.0, 164.9, 153.4, 149.6, 149.3, 146.8, 146.5, 146.2, 146.0, 145.9, 145.7, 145.1, 144.3, 142.6, 142.3, 142.0, 141.9, 139.8, 139.4, 139.1, 138.9, 138.8, 138.5, 135.3, 135.2, 134.6, 134.52, 134.46, 133.3, 132.2, 131.5, 130.4, 130.1, 129.98, 129.93, 128.7, 128.4, 128.3, 127.9, 127.8, 127.7, 127.6, 127.1, 126.8, 126.7, 126.6, 123.6, 123.4, 122.6, 122.5, 121.8, 121.2, 120.6, 120.2, 119.6, 40.4 (C-2′), 39.6 (C-1′) ppm. UV-Vis (DMF): λ_{max} (log ε) 417 (5.49), 513 (4.19), 546 (3.69), 588 (3.63), 644 (3.49) nm. HRMS-ESI(+): m/z calcd for $C_{52}H_{38}N_5O$ 748.30709 $[M + H]^+$; 748.30761 found.

2-[3-Oxo-3-(pyridin-4-yl)propan-1-yl]-5,10,15,20-tetraphenylporphyrin, ***5c***. ^{1}H NMR (300 MHz, $CDCl_3$): δ 8.84 (2H, AB system, J = 5.0 Hz, H-β), 8.81 (1H, d, J = 4.9 Hz, H-β), 8.77–8.75 (4H, m, H-β, H-2″ and H-6″), 8.62 (1H, d, J = 4.9 Hz, H-β), 8.57 (1H, s, H-3), 8.22–8.19 (4H, m, H-*o*-Ph), 8.16–8.10 (4H, m, H-*o*-Ph), 7.76–

766 (12H, m, H-*m*,*p*-Ph), 7.62 (2H, d, $J = 6.2$ Hz, H-3″ and H-5″), 3.44–3.39 (2H, m, H-2′), 3.36–3.31 (2H, m, H-1′), −2.77 (2H, s, N*H*) ppm. ^{13}C NMR (125 MHz, $CDCl_3$): δ 197.6, 150.9, 150.7, 146.8, 146.5, 146.3, 145.96, 145.9, 145.7, 145.1, 144.4, 142.8, 142.5, 142.3, 142.0, 141.9, 139.74, 139.69, 139.4, 139.1, 138.9, 138.8, 138.2, 134.6, 134.5, 134.4, 133.3, 131.0, 130.4, 130.1, 130.01, 129.96, 128.9, 128.7, 128.0, 128.3, 127.9, 127.83, 127.75, 127.68, 127.1, 126.8, 126.7, 126.6, 122.7, 122.5, 121.93, 121.85, 121.1, 121.0, 120.8, 120.7, 120.2, 119.6, 118.9, 40.5 (C-2′), 39.8 (C-1′) ppm. UV-Vis (DMF): λ_{max} (log ε) 417 (5.28), 513 (3.94), 547 (3.25), 586 (3.14), 646 (2.66) nm. HRMS-ESI(+): *m*/*z* calcd for $C_{52}H_{38}N_5O$ 748.30709 $[M + H]^+$; 748.30705 found.

Methylation of porphyrin-pyridine derivatives 1a–c: general procedure. To a solution of each porphyrin–pyridine derivatives **1a–c** (20.0 mg, 2.7×10^{-5} mol) in DMF (1 mL) in a sealed tube was added an excess of methyl iodide (60 equiv., 0.1 mL). The mixture was stirred for 24 h at 40 °C. After cooling, the crude mixture was precipitated with diethyl ether, filtered, washed with diethyl ether, dissolved in a mixture CH_2Cl_2/CH_3OH (9 : 1) and the solvent was evaporated under reduced pressure. Compounds **6a–c** were obtained without further purification by crystallisation from CH_2Cl_2/hexane in 87%, 96% and 97%, respectively. The compounds obtained were fully characterised by NMR, mass and UV-Vis techniques.

2-[2,2′:6,2″-(1′,1″-Dimethyl)terpyridinium-4-yl]-5,10,15,20-tetraphenylporphyrin di-iodide, ***6a****.* ^{1}H NMR (500 MHz, $CDCl_3$/CD_3OD): δ 9.33 (2H, d, $J = 5.9$ Hz, H-6″), 9.04 (1H, s, H-3), 8.90 (2H, AB system, $J = 4.9$ Hz, H-β), 8.83 (1H, d, $J = 4.9$ Hz, H-β), 8.79 and 8.77 (2H, AB system, $J = 4.9$ Hz, H-β), 8.75 (1H, d, $J =$ 4.9 Hz, H-β), 8.63 (2H, t, $J = 7.9$ Hz, H-4″), 8.26–8.24 (4H, m, H-*o*-Ph and H-3″) 8.21–8.17 (6H, m, H-*o*-Ph), 8.13 (2H, s, H-3′ and H-5′), 7.78–7.71 (9H, m, H-*m*,*p*-Ph), 7.49–7.47 (2H, m, H-5″), 7.31–7.29 (3H, m, H-*m*,*p*-Ph), 4.58 (6H, s, *N*-CH_3) ppm. ^{13}C NMR (125 MHz, $CDCl_3/CD_3OD$): δ 152.7, 151.1, 148.5, 148.3, 146.2, 141.6, 141.4, 141.3, 137.1, 134.9, 134.8, 134.7, 133.9–133.3 (C-β), 131.84, 131.80, 130.6, 129.9, 129.3, 129.0, 128.9, 128.6, 128.3, 128.1, 127.2, 127.1, 127.0, 121.4, 120.9, 119.7, 50.2 ppm. UV-Vis (DMF): λ_{max} (log ε) 422 (4.95), 518 (3.48), 553 (3.37), 595 (3.31), 653 (3.19) nm. HRMS-ESI(+): *m*/*z* $C_{61}H_{45}N_7$ calcd for 437.68684 $[M^{2+}]$; 437.68569 found.

2-[3,2′:6,3″-(1′,1″-Dimethyl)terpyridinium-4-yl]-5,10,15,20-tetraphenylporphyrin di-iodide, ***6b****.* ^{1}H NMR (300 MHz, DMSO-d_6): δ 9.89 (2H, s, H-2″), 9.46 (2H, d, $J = 8.1$ Hz, H-6″), 9.13 (2H, d, $J =$ 6.0 Hz, H-4″), 8.94–8.74 (7H, m, H-β), 8.42 (2H, s, H-3′and H-5′), 8.36–802 (10H, m, H-*o*-Ph and H-5″), 7.87–7.79 (9H, m, H-*m*,*p*-Ph), 7.18–7.07 (3H, m, H-*m*,*p*-Ph), 4.53 (6H, s, *N*-CH_3), −2.74 (2H, s, N*H*) ppm. ^{13}C NMR (125 MHz, DMSO-d_6): 162.3, 149.0, 148.8, 145.6, 144.0, 142.2, 141.2, 141.1, 140.7, 139.6, 137.1, 137.0, 135.8, 134.3, 134.2, 134.1, 132.0, 128.3, 128.2, 128.1, 127.8, 127.7, 127.6, 127.2, 127.1, 126.7, 126.1, 125.6, 123.6, 123.5, 120.9, 120.50, 120.45, 120.3, 120.2, 44.2 ppm. UV-Vis (DMF): λ_{max} (log ε) 423 (4.89), 518 (3.50), 554 (3.04), 597 (3.22), 649 (3.07) nm. HRMS-ESI(+): *m*/*z* for $C_{61}H_{45}N_7$ calcd for 437.68694 $[M^{2+}]$; 437.68507 found.

2-[4,2′:6,4″-(1′,1″-Dimethyl)terpyridinium-4-yl]-5,10,15,20-tetraphenylporphyrin di-iodide, ***6c****.* ^{1}H NMR (300 MHz, DMSO-d_6): δ 9.16 (4H, d, $J = 6.8$ Hz, H-2″ and H-6″), 9.01 (4H, d, $J = 6.8$ Hz, H-3″ and H-5″), 8.95–8.80 (7H, m, H-β), 8.66 (2H, s, H-3′and H-5′), 8.27–8.05 (8H, m, H-*o*-Ph), 7.86–7.81 (9H, m, H-*m*,*p*-Ph), 7.10–7.00 (3H, m, H-*m*,*p*-Ph), 4.45 (6H, s, N-CH_3), −2.75 (2H, s, N*H*) ppm. ^{13}C NMR (125 MHz, DMSO-d_6): δ 162.3, 151.5, 149.4, 146.1, 145.3, 141.2, 141.1, 140.8, 139.7, 135.8, 134.3, 134.2, 132.8–129.8 (C-β), 127.2, 127.1, 126.2, 126.1, 124.5, 120.8, 120.5, 120.3, 47.6 (*C*H_3) ppm. UV-Vis (DMF): $\lambda_{máx}$ (log ε) 423 (4.89), 518 (3.52), 554 (3.40), 597 (3.30), 649 (3.18) nm. HRMS-ESI(+): *m*/*z* for $C_{61}H_{45}N_7$ calcd for 437.68684 $[M^{2+}]$; 437.68495 found.

Ethylation of porphyrin–pyridine derivatives 1b, c: general procedure. To a solution of each porphyrin–pyridine derivatives **1** (20.0 mg, 2.7×10^{-5} mol) in DMF (1 mL) in a sealed tube was added an excess of ethyl iodide (60 equiv., 0.1 mL). The mixture was stirred for 24 h at 40 °C. After cooling, the crude mixture was precipitated with diethyl ether, filtered, washed with diethyl ether, dissolved in a mixture CH_2Cl_2/CH_3OH (9 : 1) and the solvent was evaporated under reduced pressure. Compounds **7b** and **7c** were obtained without further purification by crystallisation from CH_2Cl_2/hexane in 96% and 95%, respectively. The compounds obtained were fully characterised by NMR, mass and UV-Vis techniques.

2-[3,2′:6,3″-(1′,1″-Di-ethyl)terpyridinium-4-yl]-5,10,15,20-tetraphenylporphyrin di-iodide, ***7b****.* ^{1}H NMR (300 MHz, DMSO-d_6): δ 9.91 (2H, s, H-2″), 9.51 (2H, d, $J = 8.3$ Hz, H-6″), 9.26 (2H, d, $J =$ 6.1 Hz, H-4″), 8.95–8.80 (7H, m, H-β), 8.45 (2H, s, H-3′ and H-5′), 8.39 (2H, dd, $J = 6.1$ and 8.3 Hz, H-5″), 8.27–808 (8H, m, H-*o*-Ph), 7.88–7.83 (9H, m, H-*m*,*p*-Ph), 7.16–7.09 (3H, m, H-*m*,*p*-Ph), 4.82 (4H, q, $J = 7.2$ Hz, CH_2CH$_3$), 1.67 (6H, t, $J = 7.2$ Hz, CH$_2$CH_3), −2.74 (2H, s, N*H*). ppm. ^{13}C NMR (125 MHz, DMSO-d_6): δ 151.9, 149.5, 145.1, 141.2, 141.1, 140.8, 139.7, 135.9, 134.30, 134.26, 134.20, 133.2–130.2 (C-β), 128.3, 128.0, 127.2, 127.1, 126.3, 126.1, 125.0, 120.8, 120.5, 120.3, 56.0 (*C*H_2CH$_3$), 16.4 (*C*H_2-CH$_3$) ppm. UV-Vis (DMF): $\lambda_{máx}$ (log ε) 423 (4.72); 518 (3.81); 552 (3.39); 595 (3.25); 651 (3.18) nm. HRMS-ESI(+): *m*/*z* for $C_{63}H_{49}N_7$ calcd for 451.70249 $[M^{2+}]$; 451.70106 found.

2-[4,2′:6,4″-(1′,1″-Di-ethyl)terpyridinium-4-yl]-5,10,15,20-tetraphenylporphyrin di-iodide, ***7c****.* ^{1}H NMR (300 MHz, DMSO-d_6): δ 9.29 (4H, d, $J = 6.8$ Hz, H-2″ and H-6″), 9.04 (H, d, $J = 6.8$ Hz, H-3″ and H-5″), 8.95–8.80 (7H, m, H-β), 8.68 (2H, s, H-3′ and H-5′), 8.026–8.06 (8H, m, H-*o*-Ph), 7.88–7.83 (9H, m, H-*m*,*p*-Ph), 7.11–7.04 (3H, m, H-*m*,*p*-Ph), 4.74 (4H, q, $J = 7.2$ Hz, CH_2CH$_3$), 1.65 (6H, t, $J = 7.2$ Hz, CH$_2$CH_3), −2.74 (2H, s, N*H*) ppm. ^{13}C NMR (125 MHz, DMSO-d_6): δ 150.0, 149.1, 144.6, 143.1, 142.7, 141.2, 141.1, 140.8, 139.7, 137.5, 135.9, 134.30, 134.28, 134.17, 133.3–130.3 (C-β), 128.5, 128.4, 128.3, 128.2, 128.1, 127.2, 127.1, 126.1, 123.7, 120.9, 120.6, 120.33, 120.26, 57.0 (*C*H_2CH$_3$), 16.6 (*C*H_2CH$_3$) ppm. UV-Vis (DMF): $\lambda_{máx}$ (log ε) 423 (4.88); 519 (3.63); 554 (3.28); 596 (3.11); 652 (3.05) nm. HRMS-ESI(+): *m*/*z* for $C_{63}H_{49}N_7$ calcd for 451.70249 $[M^{2+}]$; 451.70119 found.

Electrospray ionization mass studies

Electrospray ionization mass spectra were acquired with a Micromass Q-Tof 2 (Micromass, Manchester, UK), operating in the positive ion mode, equipped with a Z-spray source, an electrospray probe and a syringe pump. Source and desolvation temperatures were 80 °C and 150 °C, respectively. Capillary

voltage was 3000 V. The spectra were acquired at a nominal resolution of 9000 and at cone voltages of 30 V. Nebulisation and collision gases were N_2 and Ar, respectively. Porphyrin solutions in methanol were introduced at a 10 μL min^{-1} flow rate.

Theoretical calculations

All calculations were performed with Gaussian09 using Density Functional Theory with the B3LYP functional and the 6-311G(d,p) basis set. Default optimization parameters were used throughout the calculations. Vibrational analysis was performed to assess the nature of the optimized structures and to determine the zero-point energy corrections.

All geometry optimized structures show positive vibration frequencies.

Singlet oxygen generation

Stock solution of each porphyrin derivative at 0.1 mM in DMF and a stock solution of 1,3-diphenylisobenzofuran (DPiBF) at 10 mM in DMF were prepared. Aliquots of 2 mL of a solution of each porphyrin (0.5 μmol dm^{-3}) and 1,3-diphenylisobenzofuran (DPiBF, 50 μmol dm^{-3}) in DMF/H_2O (9 : 1) were irradiated at an irradiance of 4.0 mW cm^{-2}, in a glass cuvette, at room temperature and under gentle magnetic stirring, with a home-made red LED array in order to prevent the photodegradation of DPiBF. The LED array is composed of a matrix of 5 × 5 LED that makes a total of 25 light sources with an emission peak at 630 nm and a bandwidth at half maximum of ± 20 nm. The absorption decay of DPiBF at 415 nm was measured at irradiation intervals up to 10 min. The production of singlet oxygen was evaluated qualitatively through the DPiBF, a singlet oxygen ($^1O_2$) quencher, due to the fact that DPiBF decays in a first order manner during continuous irradiation in a photosensitised experiments. The irradiation of the PS in the presence of dissolved oxygen will result in the formation of $^1O_2$, which is trapped by DPiBF resulting in colourless *o*-dibenzoylbenzene, after the Diels–Alder like reaction with $^1O_2$.[50]

Biologic evaluation studies

Photosensitizer stock solutions. Stock solutions of each porphyrin derivative at 500 μM was prepared in DMSO and stored in the dark. Before each assay, the PS solution was sonicated for 30 min at room temperature.

Light sources. The photodynamic effect of the cationic PS was evaluated by exposing the bacterial suspension in the presence of PS to a set of fluorescent PAR lamps or a halogen lamp. The first light source is constituted by 13 fluorescent lamps OSRAM 21 of 18 W each one, PAR radiation (380–700 nm) at an irradiance of 4.0 mW cm^{-2}. The second light source used is comprised by an illumination system (LumaCare®, USA, model LC122) equipped with a halogen 250 W quartz type lamp and coupled to an interchangeable fibre optic probe (400–800 nm). This illumination system was used to irradiate the microcosm's setup with white light (400–800 nm) at an irradiance of 150 mW cm^{-2}. All the irradiances were measured with a Power Meter Coherent FieldMaxII-Top combined with a Coherent PowerSens PS19Q energy sensor.

Bacterial strains and growth conditions. Bioluminescent *E. coli* was grown on tryptic soy agar (TSA, Merck) supplemented with 50 mg mL^{-1} of ampicillin (Amp) and with 45 mg mL^{-1} of chloramphenicol (Cm), and stored at −80 °C in 10% glycerol. Before each assay, one isolated colony was aseptically transferred to 30 mL of triptic soy broth (TSB, Merck) medium previously added with both antibiotics (150 μL Amp/100 mL TSB and 60 μL Cm/100 mL TSB) and was grown overnight at 25 °C under stirring (120 rpm). Afterwards, an aliquot was transferred into fresh TSB under the same growth conditions to reach stationary growth phase. An *E. coli*, an optical density at 600 nm (OD_{600}) of 1.6 ± 0.1 corresponded to ≈10^8 colony forming units (CFU) per mL.

Bioluminescence *versus* colony forming units. The correlation between CFUs and the bioluminescent signal (in RLUs) of bioluminescent *E. coli* strain was evaluated. Therefore, the bacteria were grown under the aforementioned conditions. Fresh overnight bacterial culture was serially diluted (10^{-1} to 10^{-5}) in PBS. Non-diluted (10°) and diluted aliquots were pour-plated on TSA medium (0.5 mL) and, simultaneously, were read on a luminometer (0.5 mL) (TD-20/20 Luminometer, Turner Designs, Inc., Madison, WI, USA) to determine the bioluminescence signal.

Photosensitization procedure. Bacterial culture grown overnight and tenfold diluted in phosphate buffered saline (PBS) was equally distributed in sterilized and acid-washed beakers. Afterwards, the appropriate volumes of each cationic porphyrin (**6a**, **6b** and **6c**) were added to achieve a final desired concentration (total volume in the beakers was 15 mL per beaker). The samples were protected from light with aluminium foil and remained in the dark for 10 min to promote the porphyrin binding to *E. coli* cells.

Light and dark controls were also carried out simultaneously with the PDI procedure: the light control (LC) comprised a bacterial suspension exposed to the same light protocol; and the dark control (DC) comprised a bacterial suspension incubated with PS at the maximum studied concentration but protected from light. Three independent experiments were performed and, for each, two replicates were plated. Both controls were carried out during each experiment.

Irradiation conditions. The samples were exposed to light under stirring and placed on a tray with clamps and the bottom of the tray was covered with water in order to maintain the samples at constant temperature (25 °C). For the PAR white light irradiation at an irradiance of 4.0 mW cm^{-2} aliquots of 1.0 mL treated and control samples were collected at time 0 and after 30, 90, 120, 180 and 270 min of light exposure and the bioluminescence signal was measured in the luminometer. For the white light at an irradiance of 150 mW cm^{-2} aliquots of 1.0 mL were collected from treated and control samples and the bioluminescence signal was measured in the luminometer at time 0 and after each 15 min until a total of 210 min. Three independent experiments were performed in two replicates and the results were averaged.

The compounds **6a–c** at concentration of 20 μM were irradiated with white light at an irradiance of 4.0 mW cm^{-2} while compound **6a** was also tested at final concentrations of 5, 10 and 40 μM. Compound **6a** at 20 μM was irradiated with white light at an irradiance of 150 mW cm^{-2} with the Lumacare® System.

Acknowledgements

Thanks are due to FCT/MEC for the financial support to the QOPNA research Unit (FCT UID/QUI/00062/2013), the CESAM (UID/AMB/50017/2013), CICECO-Aveiro Institute of Materials, POCI-01-0145-FEDER-007679 (FCT Ref. UID/CTM/50011/2013), through national funds and when applicable co-financed by the FEDER, within the PT2020 Partnership Agreement and "Compete" 2020, and also to the Portuguese NMR Network. Scientific PROTEOMASS Association (Portugal) and the Associate Laboratory for Green Chemistry LAQV (FCT/MEC (UID/QUI/50006/2013) and PT2020-POCI-01-0145-FEDER-007265) and the Unidade de Ciências Biomoleculares Aplicadas-UCIBIO (FCT/MEC (UID/Multi/04378/2013) and PT2020-POCI-01-0145-FEDER-007728) for general funding. Nuno M M Moura and Catarina I V Ramos thank FCT for their Post-Doc scholarships SFRH/BPD/84216/2012 and SFRH/BPD/85902/2012, respectively. Sérgio M Santos thanks FCT for the FCT Investigator starting grant IF/00973/2014.The authors wish to express their appreciation to Dr M Graça O Santana-Marques (Department of Chemistry, University of Aveiro, Portugal) for all the helpful and valuable suggestions. Finally, we would like to thank MSc Bárbara Coelho and graduation students Rafael Queirós Fernandes and Selesa Vanessa Shabudin for their help in the synthesis of some of the compounds described.

References

1 K. M. Kadish, K. M. Smith and R. Guilard, in *Handbook of Porphyrin Science*, World Scientific Publishing Company, Singapore, 2010, vol. 10–12.
2 B. R. Patel and K. S. Suslick, *J. Am. Chem. Soc.*, 1998, **120**, 11802.
3 M. Yu, Y. J. Zhang, J. H. Shi, G. F. Liu and H. J. Zhang, *Solid State Sci.*, 2009, **11**, 2016.
4 M. Ethirajan, Y. Chen, P. Joshi and R. K. Pandey, *Chem. Soc. Rev.*, 2011, **40**, 340 and references herein cited.
5 H. Abrahamse and M. R. Hamblin, *Biochem. J.*, 2016, **473**, 347–364.
6 H.-G. Jeong and M.-S. Choi, *Isr. J. Chem.*, 2016, **56**, 110.
7 A. B. Ormond and H. S. Freeman, *Materials*, 2013, **6**, 817.
8 E. Alves, M. A. F. Faustino, M. G. P. M. S. Neves, Â. Cunha, H. Nadais and A. Almeida, *J. Photochem. Photobiol., C*, 2015, **22**, 34 and references herein cited.
9 D. M. Adolfo Vera, M. H. Haynes, A. R. Ball, T. Dai, C. Astrakas and M. J. Kelso, *Photochem. Photobiol.*, 2012, **88**, 499.
10 T. G. S. Denis, T. Dai, L. Izikson, C. Astrakas, R. R. Anderson, M. R. Hamblin and G. P. Tegos, *Virulence*, 2011, **2**, 509.
11 M. Tim, *J. Photochem. Photobiol., B*, 2015, **150**, 2.
12 R. Weijer, M. Broekgaarden, M. Kos, R. van Vught, E. A. J. Rauws, E. Breukink, T. M. van Gulik, G. Storm and M. Heger, *J. Photochem. Photobiol., C*, 2015, **23**, 103.
13 L. R. Pereira and F. C. da Silva, *J. Med. Microb. Diagn.*, 2014, **3**, 158.
14 F. F. Sperandio, Y.-Y. Huang and M. R. Hamblin, *Recent Pat. Anti-Infect. Drug Discovery*, 2013, **8**, 108.
15 T. Maisch, R.-M. Szeimies, G. Jori and C. Abels, *Photochem. Photobiol. Sci.*, 2004, **3**, 907.
16 S. Perni, P. Prokopovich, J. Pratten, I. P. Parkin and M. Wilson, *Photochem. Photobiol. Sci.*, 2011, **10**, 712.
17 A. Tavares, C. M. B. Carvalho, M. A. Faustino, M. G. P. M. S. Neves, J. P. C. Tomé, A. C. Tomé, J. A. S. Cavaleiro, Â. Cunha, N. C. M. Gomes, E. Alves and A. Almeida, *Mar. Drugs*, 2010, **8**, 91.
18 L. Costa, J. P. C. Tomé, M. G. P. M. S. Neves, A. C. Tomé, J. A. S. Cavaleiro, M. A. F. Faustino, Â. Cunha, N. C. M. Gomes and A. Almeida, *Antiviral Res.*, 2011, **91**, 278.
19 E. Alves, M. A. F. Faustino, M. G. P. M. S. Neves, Â. Cunha, J. P. C. Tomé and A. Almeida, *Future Med. Chem.*, 2014, **6**, 141.
20 R. J. Simmons, R. D. Griffith, L. A. Falto-Aizpurua and K. Nouri, *J. Eur. Acad. Dermatol. Venereol.*, 2015, **29**, 1275.
21 M. Rajendran, *Photodiagn. Photodyn. Ther.*, 2016, **13**, 175.
22 E. Alves, A. C. Esteves, A. Correia, Â. Cunha, M. A. F. Faustino, M. G. P. M. S. Neves and A. Almeida, *Photochem. Photobiol. Sci.*, 2015, **14**, 1169.
23 D. Mostafa and B. Tarakji, *J. Clin. Med. Res.*, 2015, **7**, 393.
24 A. Srivatsana, J. R. Missertb, S. K. Upadhyayc and R. K. Pandey, *J. Porphyrins Phthalocyanines*, 2015, **19**, 111.
25 M. P. Cormick, M. G. Alvarez, M. Rovera and E. N. Durantini, *Eur. J. Med. Chem.*, 2009, **44**, 1592.
26 L. Costa, M. A. F. Faustino, J. P. C. Tomé, M. G. P. M. S. Neves, A. C. Tomé, J. A. S. Cavaleiro, Â. Cunha and A. Almeida, *J. Photochem. Photobiol., B*, 2013, **120**, 10.
27 E. Alves, J. M. M. Rodrigues, M. A. F. Faustino, M. G. P. M. S. Neves, J. A. S. Cavaleiro, Z. Lin, A. Cunha, M. H. Nadais, J. P. C. Tomé and A. Almeida, *Dyes Pigm.*, 2014, **110**, 80.
28 L. Lucantoni, M. Magaraggia, G. Lupidi, R. K. Ouedraogo, O. Coppellotti, F. Esposito, C. Fabris, G. Jori and A. Habluetzel, *PLoS Neglected Trop. Dis.*, 2011, **5**, e1434.
29 C. Fabris, R. K. Ouedraogo, O. Coppellotti, R. K. Dabiré, A. Diabaté, P. Di Martino, L. Guidolin, G. Jori, L. Lucantoni, G. Lupidi, V. Martena, S. P. Sawadogo, M. Soncin and A. Habluetzel, *Acta Trop.*, 2012, **123**, 239.
30 A. Stallivieri, F. Le Guern, R. Vanderesse, E. Meledje, G. Jori, C. Frochot and S. Acherar, *Photochem. Photobiol. Sci.*, 2015, **14**, 1290.
31 R. A. Izquierdo, C. M. Barros, M. G. Santana-Marques, A. J. Ferrer-Correia, E. M. P. Silva, F. Giuntini, M. A. F. Faustino, J. P. C. Tomé, A. C. Tomé, A. M. S. Silva, G. P. M. S. Neves, J. A. S. Cavaleiro, A. F. Peixoto, M. M. Pereira and A. A. C. C. Pais, *J. Am. Soc. Mass Spectrom.*, 2007, **18**, 218.

32 E. M. P. Silva, F. Giuntini, M. A. F. Faustino, J. P. C. Tomé, M. G. P. M. S. Neves, A. C. Tomé, A. M. S. Silva, M. G. Santana-Mmarques, A. J. Ferrer-Correia, J. A. S. Cavaleiro, M. F. Caeiro, R. R. Duarte, S. A. P. Tavares, I. N. Pegado, B. d'Almeida, A. P. A. De Matos and M. L. Valdeira, *Bioorg. Med. Chem. Lett.*, 2005, **15**, 3333.

33 M. A. Mesquita, J. C. J. M. D. S. Menezes, S. M. G. Pires, M. G. P. M. S. Neves, M. M. Q. Simões, A. C. Tomé, J. A. S. Cavaleiro, Â. Cunha, A. L. Daniel-da-Silva, A. Almeida and M. A. F. Faustino, *Dyes Pigm.*, 2014, **110**, 123.

34 M. A. Mesquita, J. C. J. M. D. S. Menezes, M. G. P. M. S. Neves, A. C. Tomé, J. A. S. Cavaleiro, Â. Cunha, A. Almeida, S. Hackbarth, B. Röder and M. A. F. Faustino, *Bioorg. Med. Chem. Lett.*, 2014, **24**, 808.

35 N. M. M. Moura, M. A. F. Faustino, M. G. P. M. S. Neves, F. A. A. Paz, A. M. S. Silva, A. C. Tomé and J. A. S. Cavaleiro, *Chem. Commun.*, 2012, **48**, 6142.

36 N. M. M. Moura, M. A. F. Faustino, M. G. P. M. S. Neves, A. C. Duarte and J. A. S. Cavaleiro, *J. Porphyrins Phthalocyanines*, 2012, **15**, 652.

37 C. I. V. Ramos, N. M. M. Moura, S. M. F. Santos, M. A. F. Faustino, J. P. C. Tomé, F. M. L. Amado and M. G. P. M. S. Neves, *Int. J. Mass Spectrom.*, 2015, **392**, 164.

38 C. I. V. Ramos, P. M. R. Pereira, M. G. O. Santana-Marques, R. De Paula, M. M. Q. Simões, M. G. P. M. S. Neves and J. A. S. Cavaleiro, *J. Mass Spectrom.*, 2014, **49**, 371.

39 A. S. Shaffer and F. Turecek, *J. Am. Soc. Mass Spectrom.*, 1995, **6**, 1004.

40 C. I. V. Ramos, M. G. Santana-Marques, A. J. Ferrer-Correia, V. V. Serra, J. P. C. Tomé, A. C. Tomé, M. G. P. M. S. Neves and J. A. S. Cavaleiro, *J. Am. Soc. Mass Spectrom.*, 2007, **18**, 762.

41 C. I. V. Ramos, M. G. Santana-Marques, A. J. Ferrer-Correia, C. M. Alonso, J. P. C. Tomé, A. C. Tomé, M. G. P. M. S. Neves and J. A. S. Cavaleiro, *J. Mass Spectrom.*, 2008, **43**, 806.

42 W. Spiller, H. Kliesch, D. Wöhrle, S. Hackbarth, B. Röder and G. Schnurpfeil, *J. Porphyrins Phthalocyanines*, 1998, **2**, 145.

43 C. S. Foote, *Photochem. Photobiol.*, 1991, **54**, 659.

44 E. Alves, C. M. B. Carvalho, J. P. C. Tomé, M. A. F. Faustino, M. G. P. M. S. Neves, A. C. Tomé, J. A. S. Cavaleiro, Â. Cunha, S. Mendo and A. Almeida, *J. Ind. Microbiol. Biotechnol.*, 2008, **35**, 1447.

45 C. Simões, M. C. Gomes, M. G. P. M. S. Neves, Â. Cunha, J. P. C. Tomé, A. C. Tomé, J. A. S. Cavaleiro, A. Almeida and M. A. F. Faustino, *Catal. Today*, 2016, **266**, 197.

46 L. Costa, C. M. B. Carvalho, M. A. F. Faustino, M. G. P. M. S. Neves, J. P. C. Tomé, A. C. Tomé, J. A. S. Cavaleiro, Â. Cunha and A. Almeida, *Photochem. Photobiol. Sci.*, 2010, **9**, 1126.

47 G. A. Pankey and L. D. Sabath, *Clin. Infect. Dis.*, 2004, **38**, 864.

48 NCCLS, *Methods for determining bactericidal activity of antibacterial agents*, approved guideline, NCCLS document M26-A, NCCLS, Villanova, PA, 1999.

49 W. L. F. Armarego and D. D. Perrin, *Purification of Laboratory Chemicals*, Butterworth-Heinemann, Oxford, 4th edn, 1996.

50 P. R. Ogilby, *Chem. Soc. Rev.*, 2010, **39**, 3181.